Supporting information

Chronicles of plutonium peroxides: spectroscopic characterization of a new peroxo compound of Pu(IV)

Julien Margate,[a] Simon Bayle, [a] Thomas Dumas,[b] Elodie Dalodière,[a] Christelle Tamain,[b] Denis Menut[c], Paul Estevenon,[b] Philippe Moisy,[b] Sergey I. Nikitenko,[a] Matthieu Virot [a,*]

[a]*ICSM, Univ Montpellier, CEA, CNRS, ENSCM, Marcoule, France.*
[b]*CEA, DES, ISEC, DMRC, Univ Montpellier, Marcoule, France.*
[c]*Synchrotron SOLEIL, L'Orme des Merisiers, Saint-Aubin, France.*

I. Materials and methods

Caution! Pu is an α-emitting radioisotope and standard precautions should be followed for handling this chemical element.

Synthesis of Pu(IV) peroxo complexes or compounds

Experiments involving plutonium were conducted at the Atalante Facility in Marcoule, France, according to regulated operating procedures in a dedicated glove box. The concentrated Pu(IV) solution was purified using anion exchange resin and was stabilized in approximately 2.4 M HNO_3. The isotopic composition (wt.%) consisted of 96.9% ^{239}Pu.

The brown peroxide complex was produced through two distinct methods. Initially, one method involved diluting a small volume of concentrated Pu(IV) solution with hydrogen peroxide at precise stoichiometry ([Pu] = 5 mM, pH = 1.5, H_2O_2/Pu = 0.5) under vigorous stirring. The second method entailed adding a small quantity of H_2O_2 to a Pu(IV) solution stabilized in a nitric medium, maintaining the same ratio as previously mentioned ([Pu] = 5 mM, 2 M HNO_3, H_2O_2/Pu = 0.5). The synthesis of the red peroxide complex was achieved by introducing H_2O_2 to a dilute Pu(IV) solution ([Pu] = 5 mM, 2 M HNO_3, H_2O_2/Pu = 1). The green peroxide compound was obtained by diluting a small volume of a Pu(IV) concentrated solution ([Pu] = 0.25 M, [HNO_3] = 1.5 M) in a concentrated H_2O_2 solution ([Pu] = 5 mM, pH = 1-2, H_2O_2/Pu = 10-1000). Additionally, this species was produced by further adding H_2O_2 (for H_2O_2/Pu = 0.5) to the brown peroxide complex formed at pH 1.5. Whatever the conditions, both the brown and red complexes decomposed into Pu(III) with different kinetics as a function of the concentration of the reactants (stables for a few days at most). The only solution that became stable was the green peroxide one (several months). Maximal wavelength observed for the different complexes or compounds in this study and the literature are given in the **Table S2** (**SI**). The **Figure S1a** (**SI**) compares the visible absorption spectra of the green peroxo species with the one of Pu(IV) stabilized in 1 M HNO_3. The **Figure S1b** shows for comparison the absorption spectra of the PuO_2 colloid and the hexanuclear Pu(IV) cluster observed 680 nm.[1,2]

Precipitation of the solid Pu(IV) peroxide

For the synthesis of the solid and green plutonium peroxide in nitric environment, a small volume of a concentrated Pu(IV) solution stabilized in a nitric acid medium ([Pu] = 0.25 M, [HNO_3] = 1.5 M) was added to a concentrated H_2O_2 solution to reach the solubility limit of the green plutonium compound ([Pu] > 10 mM). The precipitate was then recovered via centrifugation, followed by repeated washing with a 50:50 ethanol/water solution. Finally, the solid was dried under argon flow. Regarding the plutonium peroxide in sulfuric environment, a small volume of a concentrated Pu(IV) solution stabilized in a sulfuric acid medium ([Pu] = 0.05 M, [H_2SO_4] = 0.5 M) was added to a concentrated H_2O_2 solution, resulting in an immediate precipitation. This precipitate was washed and centrifuged twice with a 50:50 ethanol:water mixture before being dried under argon flow.

Laboratory spectroscopic characterizations

Plutonium solutions were analyzed by Vis-NIR absorption spectroscopy with 1 cm PMMA cuvettes (UV3600 Shimadzu spectrophotometer, 350-900 nm range using optic fibers). Raman spectra were achieved using a HORIBA Jobin–Yvon LabRam HR Evolution within the 300 to 2000 cm^{-1} range, employing a 532 nm excitation YAG laser with a step size of 2 cm^{-1}. Concentrated droplets or powder samples were evenly spread on a glass slide before analysis. Fourier transform infrared (FT-IR) spectra were obtained using a Bruker OPTICS VERTEX 70 spectrometer, scanning between 600 and 4000 cm^{-1} with 4 cm^{-1} increments in the ATR (Attenuated Total Reflectance) mode onto the diamond crystal. **Figure S3** provides Raman spectra of the green peroxo compound (**Figure S4** provides FTIR spectra) and **Table S3** provides the position of the observed FTIR and Raman bands and their assignments.

Powder X-ray diffraction

For X-ray diffraction analysis, a Bruker D8 diffractometer equipped with a Lynxeye detector was used. Cu Kα radiation (λ = 1.54184 Å) and Bragg-Brentano geometry were applied. The powders were immobilized in glue and set in specialized sample holders to prevent potential radioactive contamination. XRD patterns were recorded at room temperature within the range of $10° \leq 2\theta \leq 80°$, with an interval of 0.02° and a counting duration of 2 s per interval. High-purity gold (99.96%, Alpha Aesar) served as an internal standard to calibrate the observed XRD angles.

Thermal analysis (TGA)

The thermal analyses (ATG) of the peroxide powders were performed using a 449 Netzsch device. The samples were placed in alumina crucibles and involved Ar (Air Liquide) flow at 20 $mL \cdot min^{-1}$ and a heating treatment up to 800°C, employing a heating rate of 2 or 1 $°C \cdot min^{-1}$. **Figure S5** and **Table S4** summarizes the TGA analyses carried out on the peroxo compound precipitated in nitric and sulfuric media.

XAS characterizations

X-ray Absorption Spectroscopy (XAS) spectra were acquired on the MARS beamline at the SOLEIL Synchrotron Radiation Facility located in Saint-Aubin, France, operating at 6 GeV with a current of 200 mA. The optical segment of the MARS beamline was equipped with a double-crystal monochromator (DCM). To facilitate the beam collimation and eliminate higher-order harmonics, two Pt-coated mirrors were positioned before and after the DCM. Energy calibration was conducted using a Zr metal foil with the first inflection point at 17 998 eV. Plutonium samples were housed in a specific cell comprised of Teflon sample holders featuring 250 µL slots, sealed by Kapton® films on both sides. The experiments were carried out in liquid samples (solutions). The samples were positioned at a 45° angle to the incident beam. Experimental spectra were acquired in fluorescence mode utilizing a 13-element HPGe solid-state detector. Scans were performed at the Pu-L_3 edge at 18 057 eV and subsequently averaged. XAS data were extracted from the raw absorption spectra using standard methods, including normalization of the edge to an absorbance value of 1. The ionization energy (E_0) was established at the maximum of the first derivative around the absorption edge (E_0 = 18 063 eV). The absorption spectra acquired on the sampled solution after the synchrotron experiment did not show any difference with the original spectrum.

The pseudo-radial distribution functions were computed through Fourier transformation in k^3–weighted Extended X-ray Absorption Fine Structure (EXAFS) within the range of 3-16 $Å^{-1}$ using a Hanning window, employing the Athena code. Fittings of the samples were performed in R space between 1 and 5 Å using ARTEMIS code. Theoretical phase and amplitude functions were calculated using the FEFF7 code integrated into the Artemis package.

Two fitting approaches were conducted on the green species sample. The first, referred to as the "free contribution," included Pu-O contributions at short distances (*ca.* 2.2 Å), intermediate distances (peroxo oxygen, O_2^{2-} at *ca.* 2.3 Å in agreement with the distances provided by Runde et *al.* [3]), and long distances (2.4-2.5 Å). In this fitting, the three Pu-O distances, the Pu-Pu distance, the coordination number, and Debye-Waller factors were left free. The paths used in the fitting were derived from existing literature on known structures (Pu-O_{medium} and Pu-Pu from ref. [3]; Pu-O_{short} and Pu-O_{long} from ref. [4]). The second fitting was carried out based on the proposed hypothetical structure, where the coordination number was fixed, and the distances and Debye-Waller factors

were allowed to free. In this case, the considered diffusion paths were the central oxygen (Pu-μ_4O) within the tetrahedron, the two oxygens from the three peroxides (Pu-O_{peroxo}) linked to each Pu and forming the edges of the tetrahedron, the oxygen from H_2O (Pu-OH_2) completing the coordination sphere of Pu, and finally the Pu (Pu-Pu) forming the corners of the tetrahedron.

In both fitting procedures, the amplitude reduction factor S_0^2 was set to 1, and the identical energy threshold correction factor ΔE_0 was applied to all paths within each respective fitting. The agreement factor r (%) and the goodness-of-fit factor χ^2_{red} for both fittings were directly supplied by DEMETER. The structural parameters are gathered in the **Table S5** (**SI**). **Figure S6** and **Figure S7** provide the XANES and EXAFS spectra of the green peroxo compound.

II. Discussion about the thermal decomposition of the green peroxo compound

The evolution of the mass loss curve for the precipitated green peroxide compound, whether in nitric or sulfuric media, shows three decomposition domains (**Fig. S5** and **Table S4**). At first, an initial mass loss between 25 and 125 °C is observed. This mass loss is attributed to the departure of water molecules in agreement with the literature.[5,6] The second domain, occurring between 125 and 225°C in the case of the nitric medium and 125 to 500°C in the case of the sulfate medium, is attributed to the departure of peroxide ligands.[6,7] Nevertheless, the frontier between both domains is not clear and both the peroxide ligands and water molecules decompositions can simultaneously occur astride these two domains. The third and last domain is observed at 225 °C and 500 °C for the nitric and sulfuric domains, respectively.[6,7] They correspond to the decomposition of the nitrate and sulfate ligands, respectively, yielding PuO_2. Calculations demonstrated that $n(Pu)/n(NO_3^-) = 2$ and $n(Pu)/n(SO_4^{2-}) = 4$. This observation allowed to assume a +2 charge for the green peroxo compound. The number of water and peroxide ligands was then calculated by taking into account the two other domains but also the data obtained from the different laboratory and synchrotron characterizations. Finally, for the nitric medium (**Figure S5a**), a good agreement was obtained between the experimental mass of the precipitated solid and the theoretical one obtained by calculations from the thermograms of the proposed hypothetical structure $Pu_4(O_2)_6O(H_2O)_{12}(NO_3)_2$ (42.01 against 42.87 mg, respectively, in nitric medium). The adjustment of the coordinated water molecules to n=10, with the structure $Pu_4(O_2)_6O(H_2O)_{10}(NO_3)_2$ improve this correlation (42.01 mg against 41.84 mg, respectively, in nitric medium). A good structural agreement was also observed from the thermograms acquired from the sulfuric medium (7.84 mg against 7.86 mg for 12 H_2O molecules and 7.84 mg against 7.67 mg for 10 H_2O molecules, **Figure S5b**).

III. Discussion about the μ_4-O group located in the tetrahedron

The proposed hypothetical structure incorporates an O atom in the centre of a tetrahedron unit designed by four Pu atoms located at the vertex of this tetrahedral unit. The short distance observed at 2.13 Å for the Pu-μ_4O distances in this structure is questioning since the tetrahedral arrangement is also observed in the PuO_2 structure with longer distances observed at 2.33 Å. The latter crystallises in the fluorite structure consisting in a face centred cubic system occupied by tetravalent Pu cations and O^{2-} ligands located at the tetrahedral interstitial positions. In this structure, each oxygen is surrounded by four Pu cations in agreement with the hypothetical structure proposed in this study. It is worth noting that ThO_2 and UO_2 bulk oxides also crystallize in the fluorite structure. An-μ_4O distances have been reported at 2.41 Å and 2.37 Å for ThO_2 and UO_2, respectively. The structural parameters for the respective oxides are compared in the **Table S1** to the one observed for Th and U-based clusters that are composed with tetrahedron-like structures incorporating μ_4-O atoms. One can observe the strong splitting of the An-O and An-An distances observed for the different clusters when compared to the bulk oxide analogs. A similar conclusion arises for CeO_2.

Table S1: comparison of An-O and An-An distances in clusters in comparison to the analogous bulk oxides (An= U, Th, Pu or Ce).

Bulk oxides				***Clusters***			
		distances	***Ref.***			***distances***	***Ref.***
ThO_2				***$[Th_4Cl_8(O)(C_8H_{16}O_5)_3]\cdot 3CH_3CN$*** [8]			
	Th-O	2.41(2) Å	[9]		Th-O	2.34(3)-2.50(1) Å*	[8]
	Th-Th	3.97(2) Å	[9]		Th-Th	3.74(9) Å 3.93(7)-4.00(6) Å	[8]
UO_2				***$U_8Cl_{24}O_4(cp^*py)_2^{2-}$*** [10] ***$(Hpy)_2[U_8L_4Cl_{10}O_4]\cdot 10py$*** [11]			
	U-O	2.37 Å	[12]		U-O	2.24(7) Å 2.30(1)–2.49(1) Å	[10] [11]
	U-U	3.87 Å	[12]		U-U	3.85(9) Å 3.59(1)- 3.96(1) Å	[10] [11]
PuO_2				***this study***			
	Pu-O	2.33(1) Å	[1,9]		Pu-O	2.13(1) Å	this study
	Pu-Pu	3.81(1) Å	[1,9]		Pu-Pu	3.65(1) Å	this study
CeO_2	Ce-O	2.34(3) Å	[13]	***$[Ce_6(\mu_3\text{-}O)_4(\mu_3\text{-}OH)_4]^{12+}$*** [14]	Ce-O	2.22(2) Å	[14]
	Ce-Ce	3.83(1) Å	[13]		Ce-Ce	3.79(3) Å	[14]

IV. SI figures and tables

Table S2: Main absorption bands and **ε** for various plutonium species prepared in aqueous solution, nitric medium and chlorohydric medium.

Species	Medium	Main Peak (nm)	ε (L.mol^{-1}.cm^{-1})	Ref
Pu(IV)	0.5 M HCl	470	54	15
	1 M HNO_3	476		16
Brown complex	0.5 M HCl	495	266	15
	0.5 - 8 M HNO_3	496		17
	0.025 - 2 M HNO_3	494		*
Red complex	0.5 M HCl	510	500	15
	0.5 - 8 M HNO_3	506		17
	2 M	506		*
Green compound	0.02 M HNO_3	455 - 821	n/a	*
PuO_2 colloid	HNO_3	616	n/a	1,18
Hexameric Pu cluster	HNO_3	455 - 645 - 680	n/a	2,19

** Data from this study.*

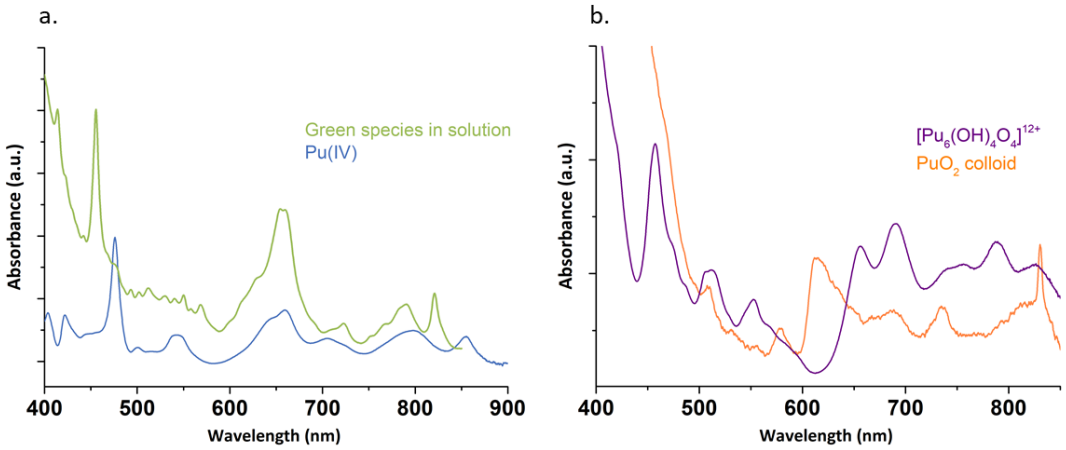

Figure S1: Vis-NIR absorption spectra acquired for (a) a Pu(IV) solution in 1 M HNO_3 (476 nm) and the green (455, 654-660 and 821 nm) peroxo species of Pu(IV) in nitric media; (b) PuO_2 colloid (616 nm) and the hexanuclear Pu(IV) cluster (455, 645 and 680 nm).

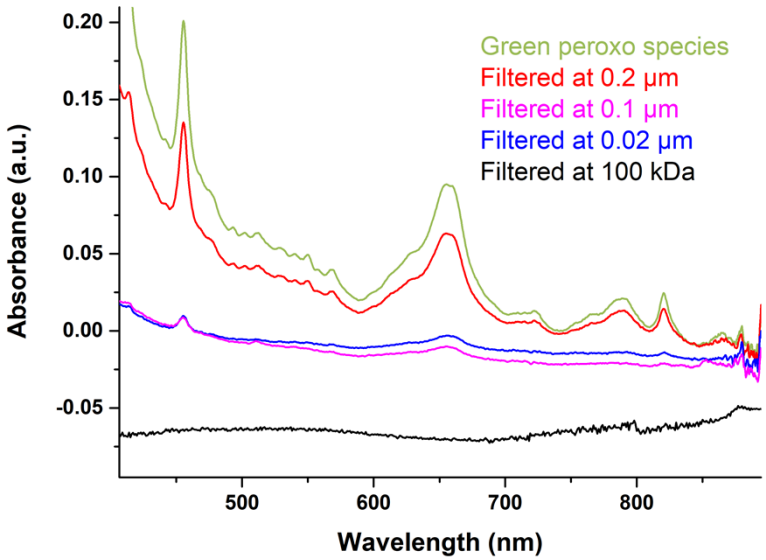

Figure S2: Vis-NIR absorption spectra of the green Pu(IV) peroxo solution ([Pu] = 1 mM, [H_2O_2] = 0.1 M) compared to the same solution successively filtered at 0.2 µm, 0.1 µm, 0.02 µm (PTFE filters) and 100 kDa (regenerated cellulose).

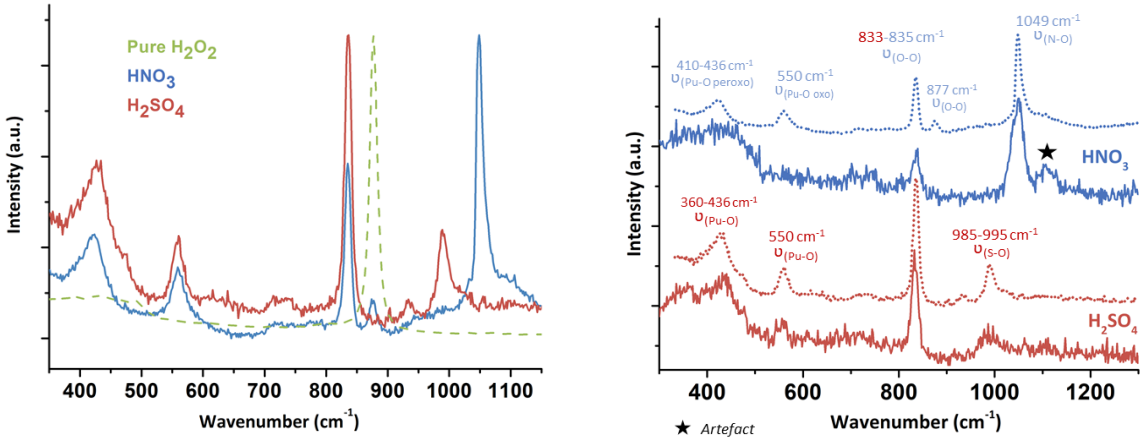

Figure S3: Raman spectra acquired (a) on concentrated droplets of the green Pu peroxo in nitric medium (blue line) and sulfuric medium (red line) (Raman spectrum of a pure H_2O_2 solution is indicated in green dot line); (b) on concentrated droplets of the Pu peroxo compound prepared in nitric (blue dot line) and sulfuric (red dot line) medium compared to the spectra acquired for the green Pu peroxo solid precipitated in nitric (blue line) and sulfuric (red line) media.

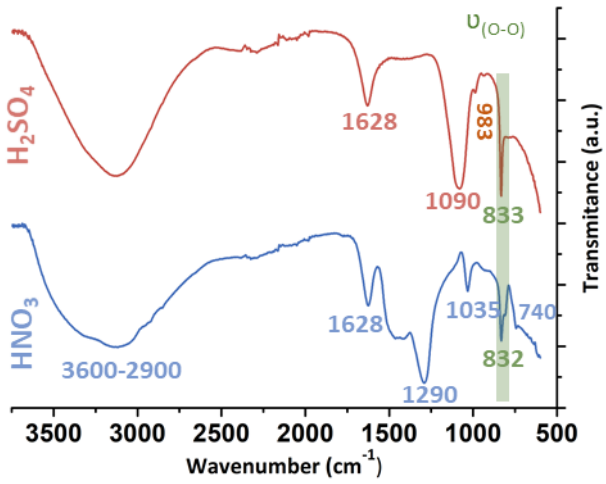

Figure S4: FT-IR spectra acquired on the green solid precipitated from nitric and sulfuric Pu(IV) solutions.

Table S3: Position and assignment of the vibrational bands of the plutonium peroxo compound in liquid droplet or solid powder form detected by FTIR and Raman spectroscopy.

Assignments	Raman shift (cm^{-1})		I.R. frequencies (cm^{-1})	
	Sulfate	Nitrate	Sulfate	Nitrate
ν(O-H)(H_2O)	-	-	3130	3130
δ(H-O-H)	-	-	1628	1628
ν(O-O)	834	834	834	832
(Pu-O_{peroxo})	421	423	-	-
Pu(O_2), Pu-O-Pu, Pu-O_{peroxo}	550	550		
ν_1(S-O)sym stretching	994	-	983	-
ν_3(S-O)asym stretch	-	-	1084	
$\nu_2(NO_3)$	-	1050	-	1026
$\nu_4(NO_3)$sym	-		-	1290
$\nu_s(NO_2)$				1452
ν_6 o.o.p rocking				800
ds(NO_2)				746

Band attribution were done based on the literature for water [20,21]*, peroxo*[22,23]*, sulfates* [24,25] *and nitrates* [26,27].

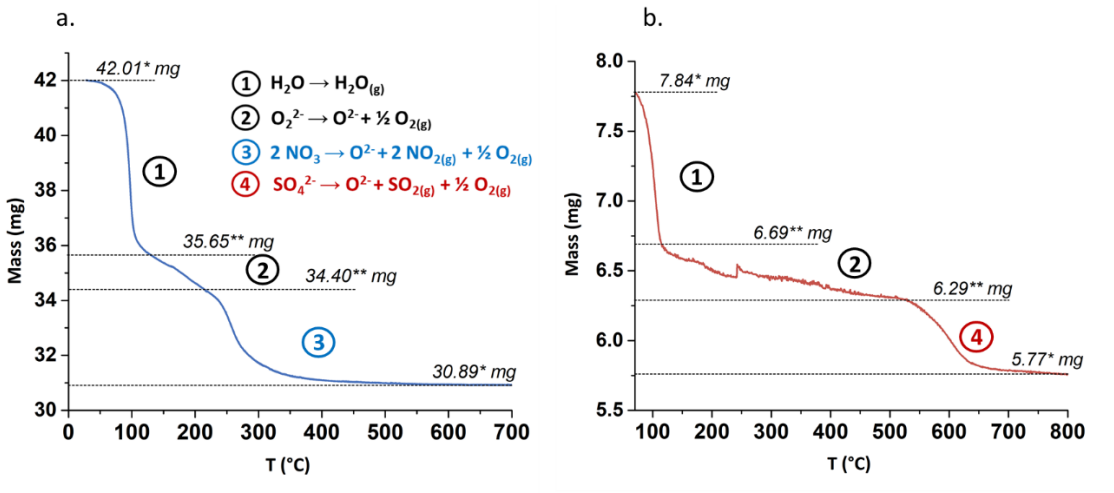

Figure S5: ATG-signals observed for the green Pu peroxo compound precipitated in (a) nitric medium, or (b) sulfuric medium. *experimental mass, **theoretical mass of the intermediate compounds obtained after derivation of the TGA signal. Three decomposition domains are proposed according to the literature.[5–7]

Table S4: Assignment of the mass losses observed during the TGA experiments performed with the green plutonium peroxo compound precipitated in (a) nitric and (b) sulfuric media.

a.

Temperature (°C)	Compound (Intermediate reaction)	Weight (mg)	$[Pu_4(O_2)_6(O)(H_2O)_{12}](NO_3)_2$ Theo. mass (mg)	Error (%)	$[Pu_4(O_2)_6(O)(H_2O)_{10}](NO_3)_2$ Theo. mass (mg)	Error (%)
25	Peroxo compound	42.01*	42.87	2 %	41.84	0.4 %
25-125	($H_2O \rightarrow H_2O_{(g)}$)	35.65**	36.71	3 %	36.71	3 %
125-225	($O_2^{2-} \rightarrow O^{2-} + ½ O_{2(g)}$)					
225-700	($2 NO_3 \rightarrow O^{2-} + 2 NO_{2(g)} + ½ O_{2(g)}$)	34.40**	33.97	1.3 %	33.97	1.3 %
800	PuO_2	30.89*	30.89*	-	30.89*	-

b.

Temperature (°C)	Compound (Intermediate reaction)	Weight (mg)	$[Pu_4(O_2)_6(O)(H_2O)_{12}](SO_4)$ Theo. mass (mg)	Error (%)	$[Pu_4(O_2)_6(O)(H_2O)_{10}](SO_4)$ Theo. mass (mg)	Error (%)
25	Peroxo compound	7.84*	7.86	0.3 %	7.67	2 %
25-125	($H_2O \rightarrow H_2O_{(g)}$)	6.69**	6.71	0.3 %	6.71	0.3 %
125-225	($O_2^{2-} \rightarrow O^{2-} + ½ O_{2(g)}$)					
225-700	($SO_4^{2-} \rightarrow O^{2-} + SO_{2(g)} + ½ O_{2(g)}$)	6.29**	6.20	1 %	6.20	1 %
800	PuO_2	5.77*	5.77*	-	5.77*	-

*experimental mass, **theoretical mass of the intermediate compounds obtained after derivation of the TGA signal.

Table S5: Structural parameters obtained by fitting the EXAFS spectrum of the green peroxo compound of Pu(IV). Data marked with an asterisk (*) were fixed.

	Path	N	σ^2 (Å^2)	R (Å)	S_0^2	E_0 (eV)	χ^2_{red}	R-factor (%)
Pu peroxide **free contribution**	Pu-Oshort	1.3 ± 0.5	0.003	2.14 ± 0.01	1	+4.5 ± 0.2	2.1	2.9
	Pu-Omedium	6.5 ± 0.6	0.004	2.32 ± 0.01				
	Pu-Olong	3.5 ± 0.7	0.002	2.45 ± 0.01				
	Pu-Pu	3.6 ± 0.7	0.005	3.65 ± 0.01				
Pu peroxide **proposed structre**	Pu-Oμ4	1*	0.002	2.13 ± 0.01	1	+1.3 ± 0.2	2.2	3.1
	Pu-Operoxo	6*	0.004	2.32 ± 0.01				
	Pu-OH_2	3*	0.002	2.45 ± 0.01				
	Pu-Pu	3*	0.004	3.65 ± 0.01				

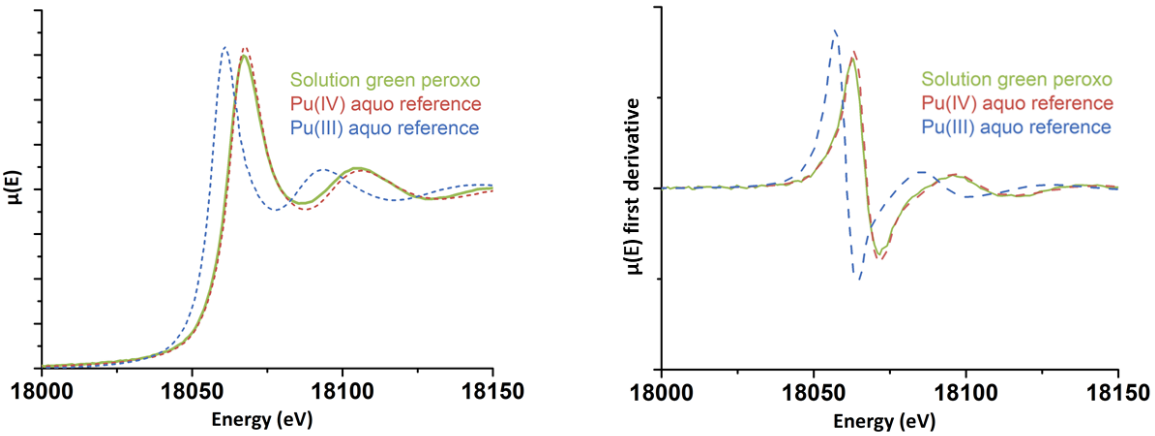

Figure S6: XANES spectra (left) and their first derivatives (right) of the green peroxo species in solution compared to Pu(IV) and Pu(III) references.

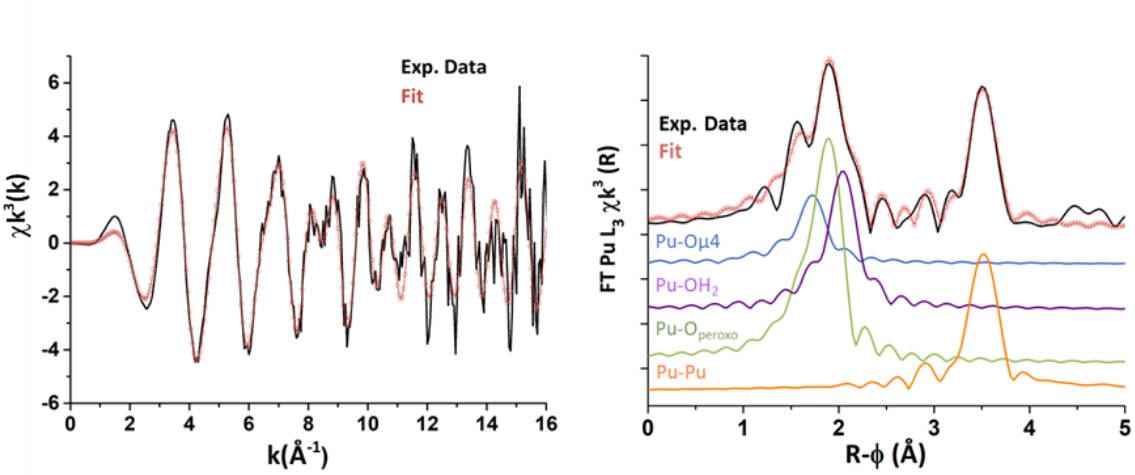

Figure S7: (left) Pu(IV) green peroxo compound raw Pu L_3-edge k^3-weighted EXAFS data, (right) FT of the experimental k^3-weighted EXAFS spectrum (black) measured on the green compound in solution (5 mM). Red circles stand for the best fit using 3 Pu-O and 1 Pu-Pu scattering paths.

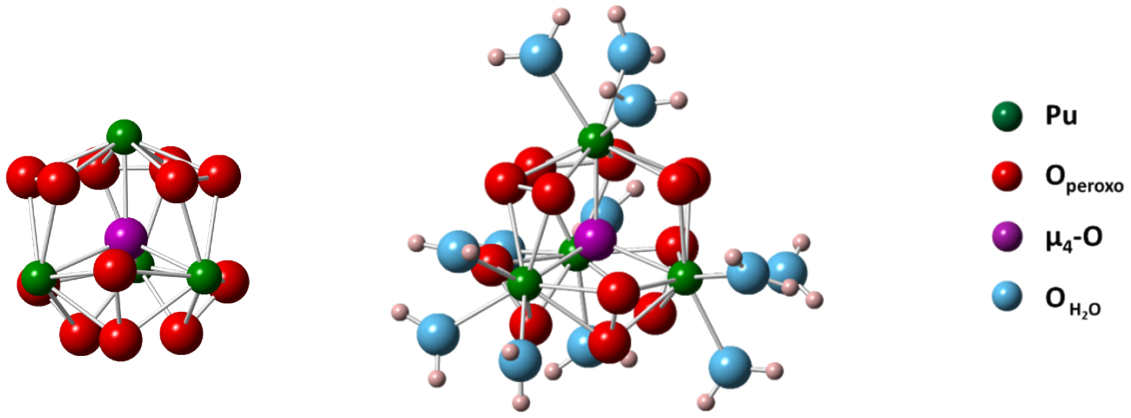

Figure S8: Structure of the hypothetical unit pattern $[Pu_4(O_2)(O)(H_2O)_{12}]_n^{2+}$ coordinated or not coordinated with water molecules. According to the filtration experiments, the green peroxo compound is not a soluble complex but rather a solid species that can aggregate or polymerize into bigger compounds. The coordinated water molecules are proposed on the single unit pattern to reach a coordination number CN= 10 for Pu but should be different on a longer scale structure.

V. References

1 M. Virot, T. Dumas, M. Cot-Auriol, P. Moisy and S. I. Nikitenko, *Nanoscale Adv.*, 2022, **4**, 4938–4971.
2 G. Chupin, C. Tamain, T. Dumas, P. L. Solari, P. Moisy and D. Guillaumont, *Inorg. Chem.*, 2022, **61**, 4806–4817.
3 W. Runde, L. F. Brodnax, G. S. Goff, S. M. Peper, F. L. Taw and B. L. Scott, *Chem. Commun.*, 2007, 1728.
4 K. E. Knope and L. Soderholm, *Chem. Rev.*, 2013, **113**, 944–994.
5 L. de Almeida, PhD, University of Lorraine, 2012.
6 N. Hibert, B. Arab-Chapelet, M. Rivenet, L. Venault, C. Tamain and O. Tougait, *Dalton Trans.*, 2022, **51**, 12928–12942.
7 J. D. Moseley and R. O. Wing, *Properties of plutonium dioxide*, 1965.
8 D. Rogers, H. Bond and M. M. Witt, .
9 L. Bonato, M. Virot, T. Dumas, A. Mesbah, E. Dalodière, O. Dieste Blanco, T. Wiss, X. Le Goff, M. Odorico, D. Prieur, A. Rossberg, L. Venault, N. Dacheux, P. Moisy and S. I. Nikitenko, *Nanoscale Adv.*, 2020, **2**, 214–224.
10 L. Moisan, T. Le Borgne, P. Thuéry and M. Ephritikhine, *Acta Crystallogr C Cryst Struct Commun*, 2002, **58**, m98–m101.
11 L. Salmon, P. Thuéry and M. Ephritikhine, *Polyhedron*, 2004, **23**, 623–627.
12 D. Prieur, P. M. Martin, A. Jankowiak, E. Gavilan, A. C. Scheinost, N. Herlet, P. Dehaudt and P. Blanchart, *Inorg. Chem.*, 2011, **50**, 12437–12445.
13 A. M. Shahin, F. Grandjean, G. J. Long and T. P. Schuman, *Chem. Mater.*, 2005, **17**, 315–321.
14 S. L. Estes, M. R. Antonio and L. Soderholm, *J. Phys. Chem*, 2016, **120**, 5810–5818.
15 R. E. Connick and W. H. McVey, *J. Am. Chem. Soc.*, 1949, **71**, 1534–1542.
16 M. Virot, L. Venault, P. Moisy and S. I. Nikitenko, *Dalton Trans.*, 2015, **44**, 2567–2574.
17 C. Maillard and J.-M. Adnet, *Radiochimica Acta*, 2001, **89**, 485–490.
18 M. Cot-Auriol, M. Virot, T. Dumas, O. Diat, D. Menut, P. Moisy and S. I. Nikitenko, *Chem. Commun.*, 2022, **58**, 13147–13150.
19 C. Tamain, T. Dumas, D. Guillaumont, C. Hennig and P. Guilbaud, *Eur. J. Inorg. Chem.*, 2016, **2016**, 3536–3540.
20 M. Falk and T. A. Ford, *Can. J. Chem.*, 1966, **44**, 1699–1707.
21 C. R. Bhattacharjee, M. K. Chaudhuri, S. K. Chettri and J. J. Laiwan, 1994, **66**, 229–231.
22 J. A. Leary, *Studies on the Preparation, Properties, and Composition of Plutonium Peroxide*, U. S. A. E. Commission and L. A. S. Laboratory, Los Alamos Scientific Laboratory of the University of California, 1954.
23 L. Bonato, M. Virot, T. Dumas, A. Mesbah, P. Lecante, D. Prieur, X. Le Goff, C. Hennig, N. Dacheux, P. Moisy and S. I. Nikitenko, *Chem. Eur. J.*, 2019, **25**, 9580–9585.
24 D. E. Chasan and G. Norwitz, *Infrared determination of inorganic sulfates and carbonates by the pellet technique :* Defense Technical Information Center, Fort Belvoir, VA, 1969.
25 K. Ben Mabrouk, T. H. Kauffmann, H. Aroui and M. D. Fontana, *J Raman Spectroscopy*, 2013, **44**, 1603–1608.
26 M. Y. Mihaylov, V. R. Zdravkova, E. Z. Ivanova, H. A. Aleksandrov, P. St. Petkov, G. N. Vayssilov and K. I. Hadjiivanov, *Journal of Catalysis*, 2021, **394**, 245–258.
27 U. Casellato, P. A. Vigato and M. Vidali, *Coordination Chemistry Reviews*, 1981, **36**, 183–265.